Supplementary Information (SI) for Analyst.

ICT-Based Fluorescent Nanoparticles for Selective Cyanide Ion Detection and Quantification in Apple Seeds

Upendar Reddy Gandra [a,b]*, Rabindranath Lo[c], Praveen B. Managutti [a,d] Abdul Mannan Butt[a], Pogula Sreekanth Reddy[e], Ahasan Ul Haq Qurashi[a,f], Sharmarke Mohamed[a,d,f], M. Infas H. Mohideen[a,f]*

[a]*Department of Chemistry, Khalifa University of Science and Technology, Abu Dhabi, P.O. Box 127788, United Arab Emirates, E-mail: upreddygandra@gmail.com*

[b]*Institute for Inorganic and Analytical Chemistry (IAAC), Friedrich Schiller University Jena, Humboldtstr. 8, D-07743 Jena, Germany.*

[c]*Institute of Organic Chemistry and Biochemistry, Czech Academy of Sciences Flemingovo nam´ ěstí 542/2, Prague 160 00, Czech Republic*

[d]*Chemical Crystallography Laboratory, Khalifa University of Science and Technology, Abu Dhabi, PO BOX 127788, United Arab Emirates.*

[e]*Center for Global Infectious Disease Research, Seattle Children's Research Institute, Seattle, WA 98109, USA.*

[f]*Center for Catalysis and Separations, Khalifa University of Science and Technology, Abu Dhabi P.O. Box 127788, United Arab Emirates. E-mail: mohamed.mohideen@ku.ac.ae*

Experimental Section:

Materials and instruments: All reagents and solvents were purchased from commercial sources and used without further purification. ^{1}H NMR spectra were recorded AV 400 MHz Bruker NMR spectrometer using $CDCl_3$-d_3 and CD_3CN-d_3 as the solvent and tetra methyl silane (TMS) as an internal standard. ESI-Ms measurements were carried out on a Waters QTof-Micro instrument. Fourier transform infrared (FTIR, VERTEX 70, Bruker) spectra were recorded to analyze the functional group. Scanning electron microscopy (SEM, JEOL JSM-7610FFEG-SEM) was employed to observe the morphology. A Perkin Elmer fluorescence spectrophotometer was used to scan and titrate fluorescence experiments. All the spectroscopy was carried out in the THF/H_2O solution. CN^- was used as the Sodium cyanide (NaCN). All measurements were carried out at ambient temperature.

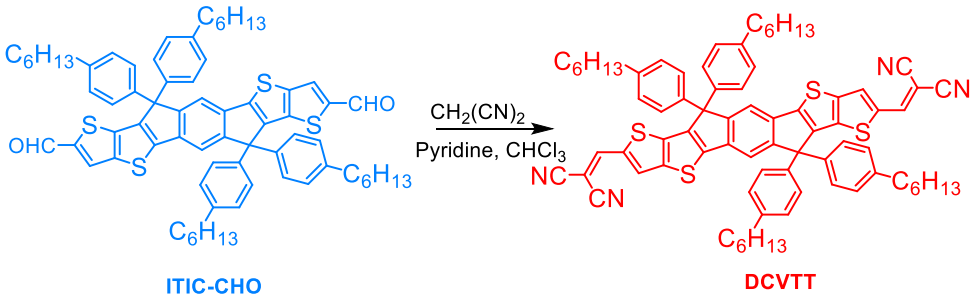

ITIC-CHO DCVTT

Scheme 1. Synthetic scheme adopted for synthesis of **DCVTT**.

Synthesis of DCVTT: ITIC-CHO (100 mg, 0.093 mmol) and malononitrile (19 mg, 0.279 mmol) were dissolved in 10 ml of dry chloroform. Pyridine (3 equivalents) was added to this reaction mixture, and the reaction mixture was stirred at 50 °C for 8 h. TLC monitored the progress of the reaction. Upon completion, the reaction mixture was allowed to room temperature. The crude reaction mixture was washed with water (30 mL) and then extracted with dichloromethane (DCM) (20 mL × 3). The crude mixture was purified by column chromatography on silica gel (ethyl acetate) to afford **DVTT** as a red compound (90 mg, 82%). ESI-MS (m/z) calculated for $C_{76}H_{72}N_4S_4$: 1170, observed: 1193 [**DVTT**+Na^+]. ^{1}H NMR (500 MHz,

$CDCl_3$) δ 7.95 (s, 2H), 7.67 (s, 2H), 7.62 (s, 2H), 7.12 (s, 16H), 2.60 – 2.53 (m, 8H), 1.58 (d, J = 6.3 Hz, 18H), 1.30 (dqd, J = 13.3, 8.8, 3.8 Hz, 26H), 0.91 – 0.83 (m, 13H). ^{13}C NMR (126 MHz, $CDCl_3$) δ 155.22, 151.71, 146.87, 143.11, 142.70, 141.94, 138.69, 136.70, 136.27, 130.81, 128.90, 127.70, 118.40, 114.39, 75.52, 63.16, 35.57, 31.68, 29.16, 22.58, 14.09. The molecular structure was validated through single crystal X-ray analysis.

General experimental procedure for UV-Vis and Fluorescence studies: $5x10^{-2}$ M solution of the NaCl, NaBr, KI, KNO_3, NaCN, $CH_3COONa.3H_2O$, $NaIO_4$, Na_2SO_3, NaF, $Na_2HPO_4.2H_2O$, $NaH_2PO_4.2H_2O$ were prepared in pure aqueous medium, A stock solution of the receptor **DCVTT** (1×10^{-4} M) was prepared in THF. For emission spectral titration, effective [CN^-] was varied between (0–100 μM). The solution of the compound **DCVTT** was further diluted with aq.-HEPES buffer: THF (1:1) for spectroscopic titrations, and the effective final concentration of the solution of compound **DCVTT** used for the fluorescence study was 20 μM. For all luminescence measurements, λ_{Ext} = 500 nm with an emission slit width of 10/10 nm.

^{1}H NMR spectra of DCVTT.

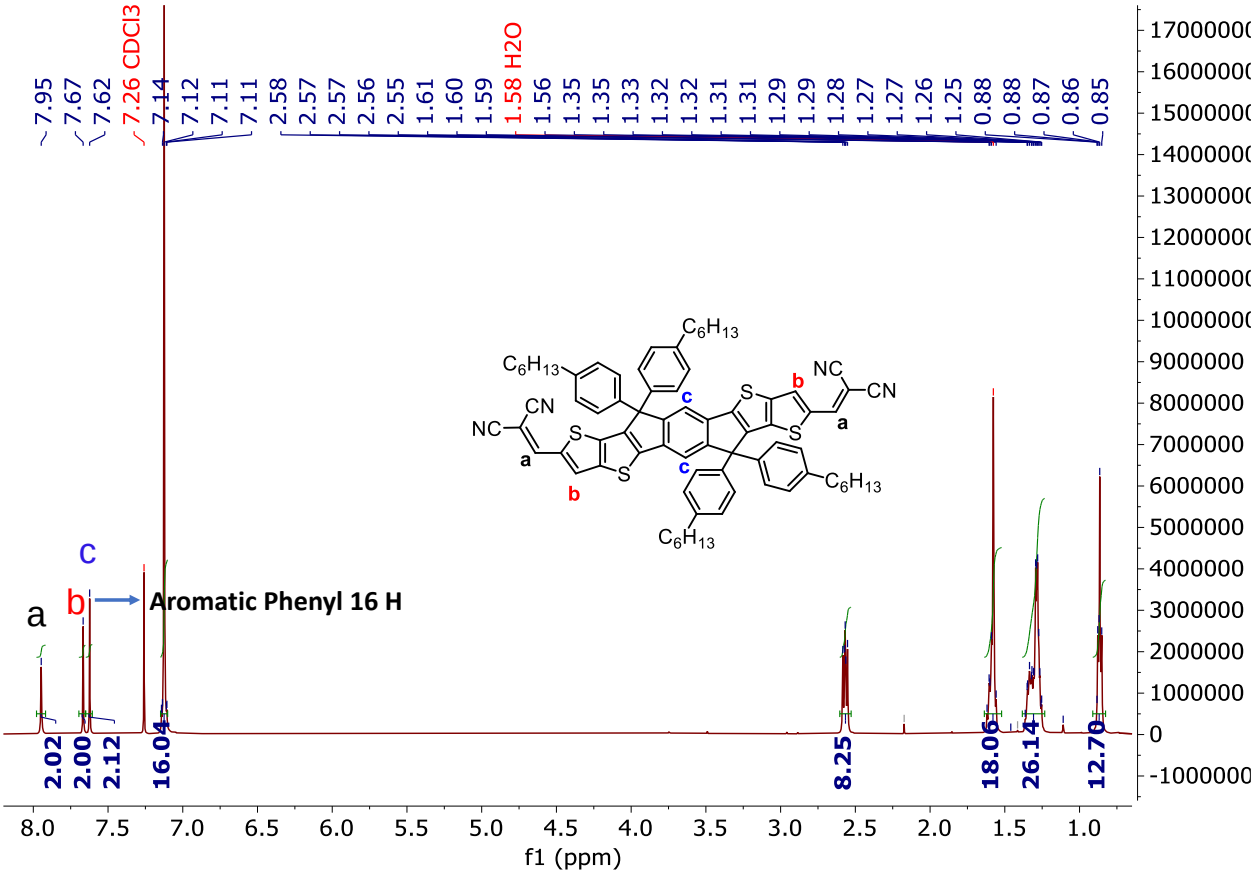

SI Figure 1: ^{1}H NMR spectra of **DCVTT** in $CDCl_3$ solvent.

^{13}C NMR spectra of DCVTT.

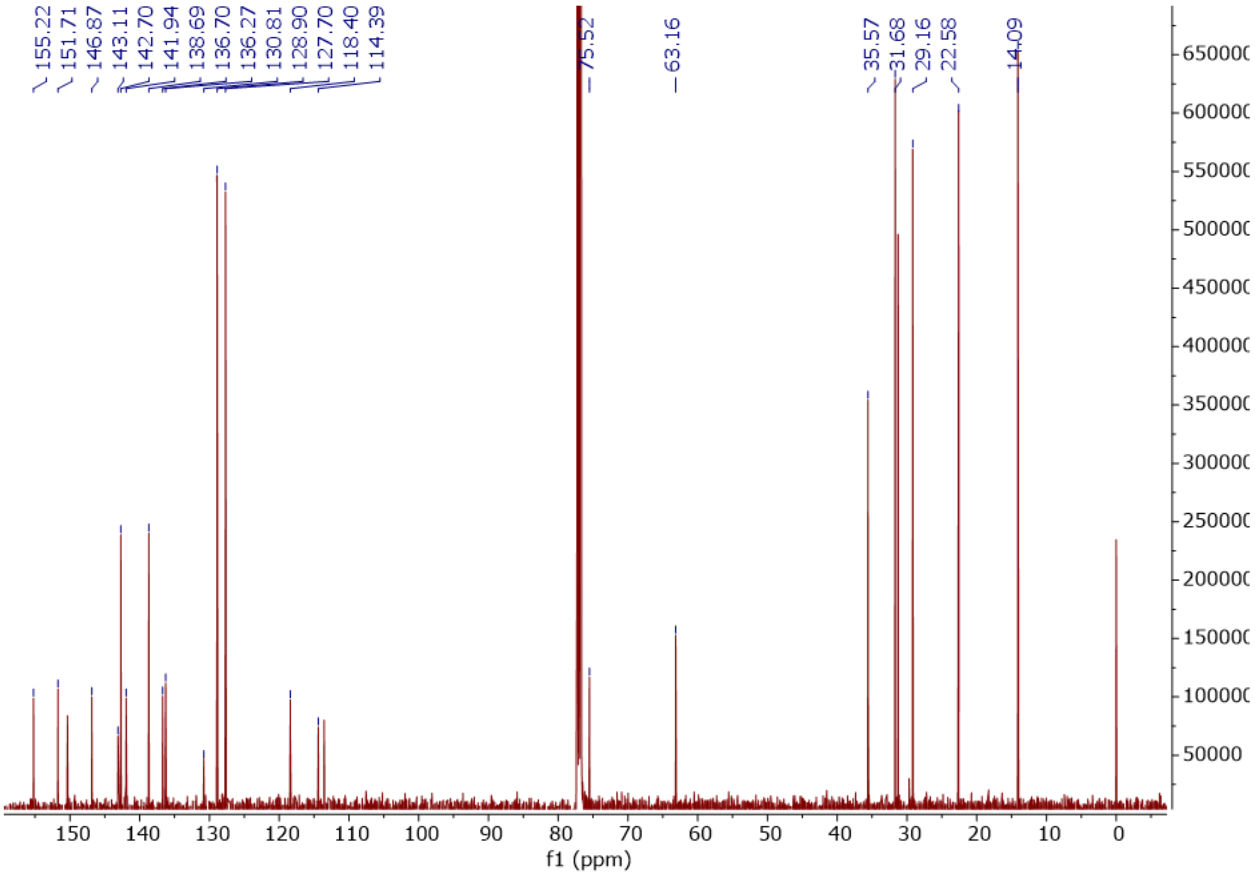

SI Figure 2: ^{13}C NMR spectra of **DCVTT** in $CDCl_3$ solvent.

ESI Mass spectra of DCVTT

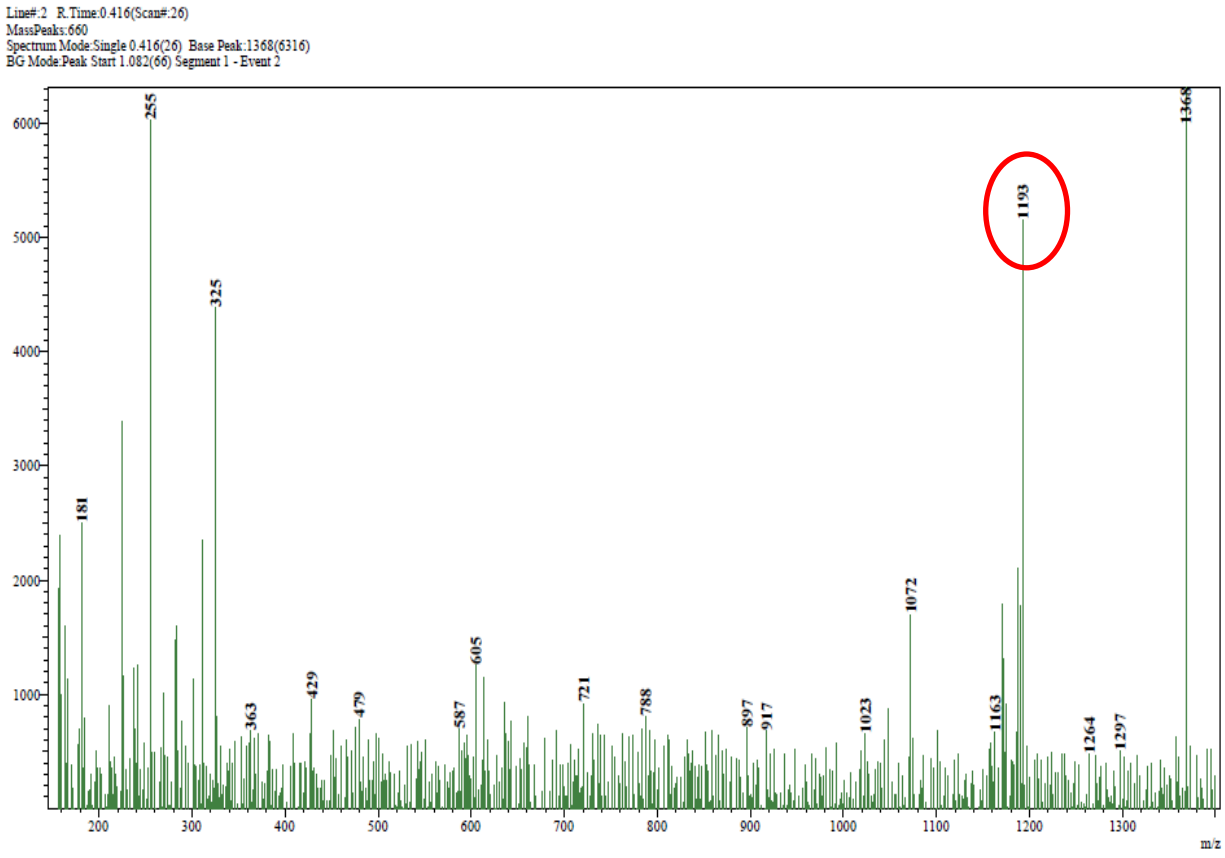

SI Figure 3: ESI- Ms spectrum of **DCVTT**.

FTIR spectrum of DCVTT

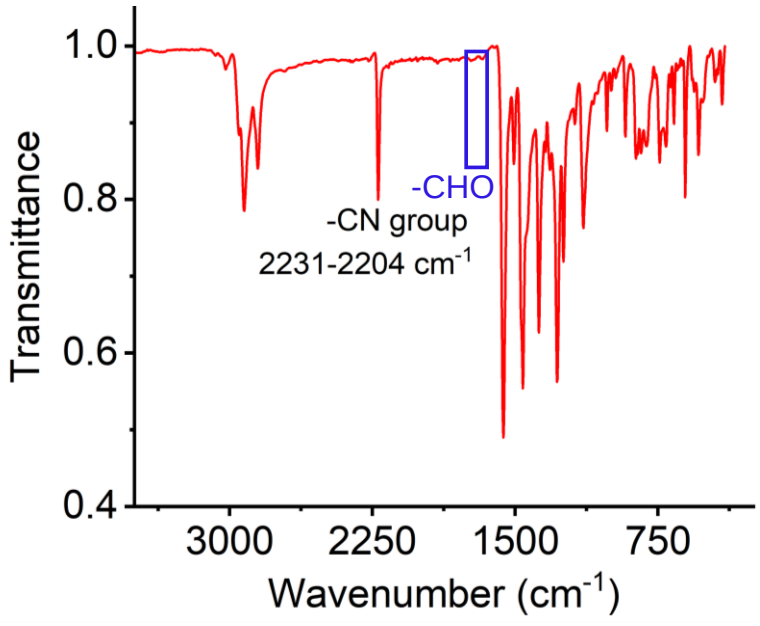

SI Figure 4: FT-IR spectrum of **DCVTT**.

Absorption spectra of DCVTT in different solvents

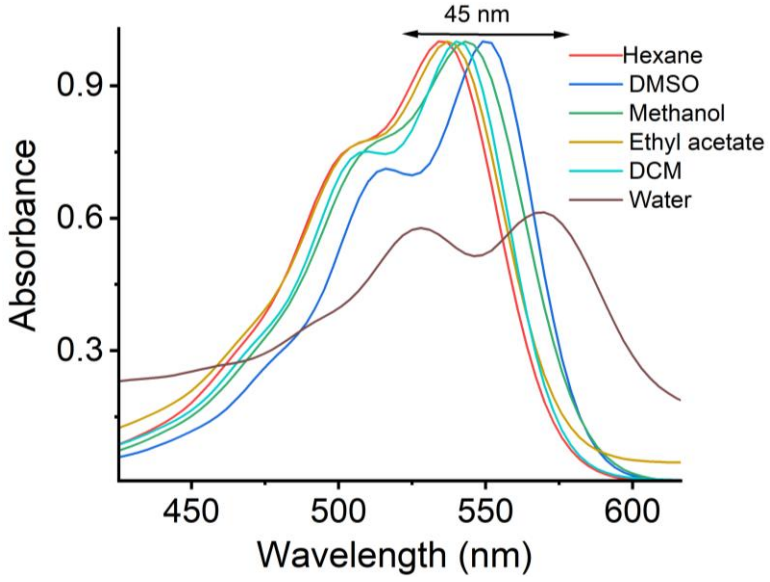

SI Figure 5: Absorption spectra of **DCVTT** in different solvents with increasing polarity.

Excitation and Emission spectra of DCVTT

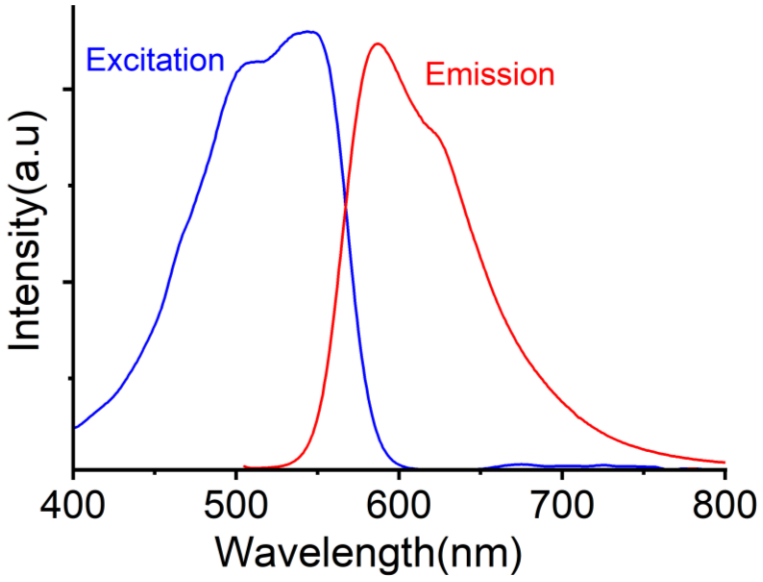

SI Figure 6: Excitation (λ_{Emiss} ^{Mon} = 595 nm) and emission (λ_{Exc}= 500 nm) spectrum of **DCVTT** recorded in THF: Water (1:1, v/v) medium.

Time-dependent fluorescence spectra of DCVTT in presence of CN^-

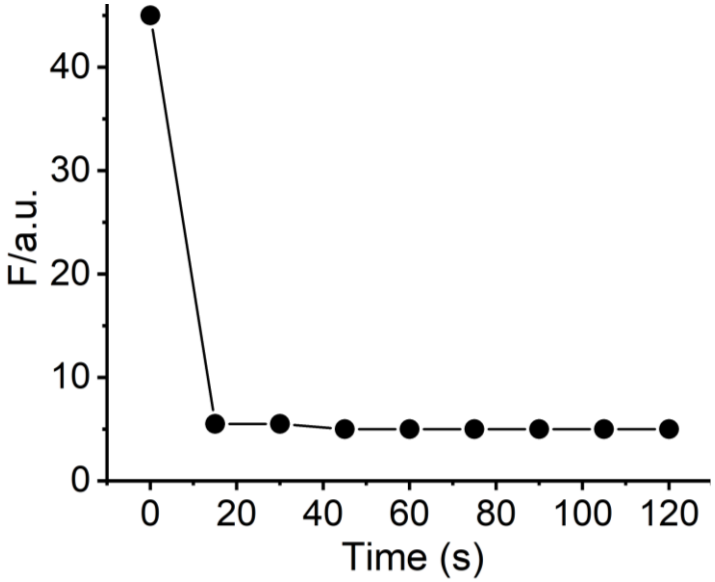

SI Figure 7: Time-dependent fluorescence spectra of **DCVTT** upon addition of an aqueous solution CN^- (40 equiv.) in THF: water (1:1) solvent.

Spectrophotometric interference study of DCVTT with CN^- in the presence of various anions

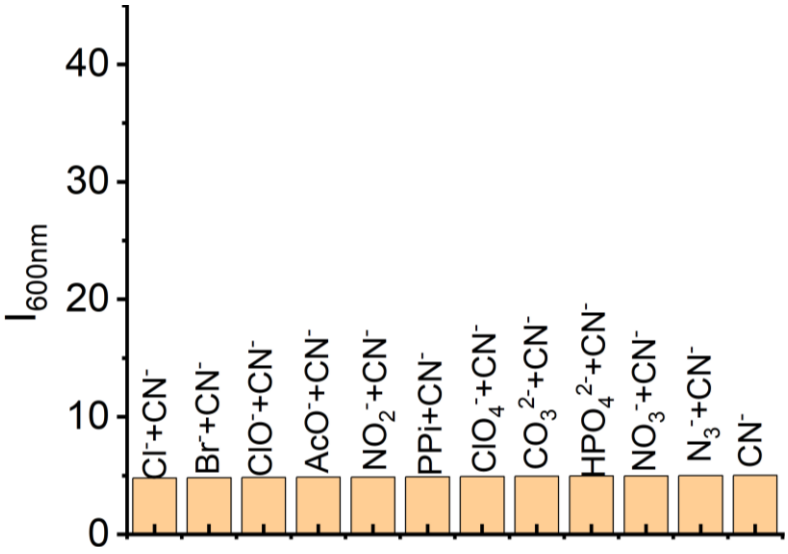

SI Figure 8: Spectrophotometric fluorescence interference study of **DCVTT** (20 μM) with CN^- (200 μM) in the presence of various anions (200 μM) in THF: water (1:1, v/v).

Change in fluorescence of DCVTT as a function of the solution pH

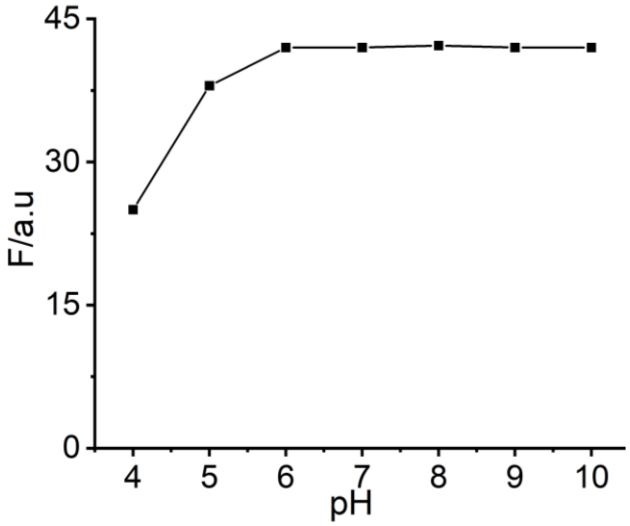

SI Figure 9: Fluorescence response of **DVTT** (20 μM) as a function of pH in THF-Universal buffer (1: 1, v/v), pH is adjusted using aqueous solutions of 1 M HCl or 1 M NaOH.

Calculation of detection limit

The detection limit was calculated based on the fluorescence titration. To determine the S/N ratio, the emission intensity of **DCVTT** without CN^- was measured 8 times, and the standard deviation of blank measurements was determined. The detection limit (DL) of **DCVTT** for CN^- was determined from the following equation:

DL = K * Sb1/S

Where K = 2 or 3 (we took 3 in this case);

Sb1 is the standard deviation of the blank solution; S is the slope of the calibration curve.

From the graph we get slope = 3.4×10^7, and Sb1 value is 0.9424

Thus, using the formula, we get the Detection Limit = 1.76×10^{-7} M.

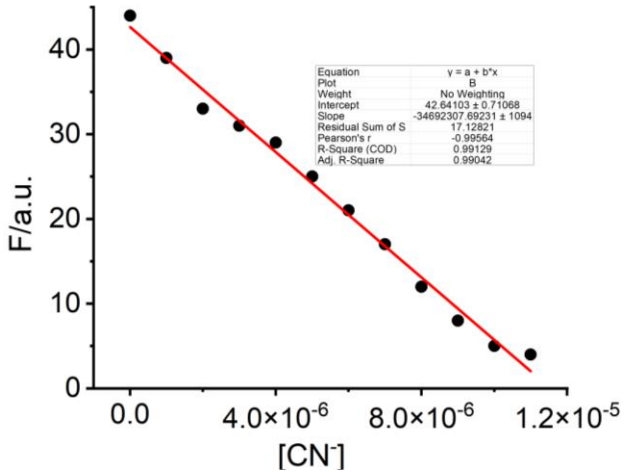

SI Figure 10: Fluorescence intensity (λ_{Ext} = 500 nm& λ_{Emiss} = 600 nm) of **DCVTT** (20 µM) upon addition of CN^- (0-100µM) in 10 mM THF: Water (1:1, v/v).

Single crystal structure of DCVTT:

Single crystal analysis: The molecule crystallizes in the monoclinic space group $P2_1/c$, as shown in SI Fig. 10a &10b. The ORTEP diagram with a 30% ellipsoid is shown in scheme 1 b. The Asymmetric unit contains one molecule of **DCVTT**, and four molecules present in the packing diagram. The packing diagram shows the ladder type of network along the *c* axis as shown in SI Fig.11 (a & b). The intramolecular hydrogen bonding N…S (3.295 Å) is shown in SI Fig. 12 along the axis. The molecules have stabilized by packing through the short π…π (3.662 Å) intermolecular interaction between the thiophene ring with each other of head and tail between the molecules. Crystal data and structure refinement for **DCVTT** are provided in SI Table 1.

The single crystals of **DCVTT (**labeled as ITIDCN in CIF. File) were crystallized from $CHCl_3$ using the slow solvent evaporation method. A suitable crystal was selected and mounted on a Rigaku Oxford Diffraction XtaLAB Synergy-S diffractometer equipped with a HyPix-6000HE Hybrid Photon Counting (HPC) detector and Cu microfocus sealed X-ray tube, as well as a low-temperature Oxford Cryosystems Cobra low-temperature device. The crystal was kept at 320.00(10) K during data collection. The data collection strategy was calculated within CrysAlisPro (Rigaku OD, 2023; Table S1) to ensure desired data redundancy and percent completeness. Using Olex2 [1], the structure was solved with the SHELXT [2] structure solution program using Intrinsic Phasing and refined with the SHELXL[3] refinement package using Least Squares minimization. The space group determination was performed by using PLATON. [4] ORTEP diagrams were generated using ORTEP-3. [5] All non-hydrogen atoms were in difference-Fourier maps and were then refined anisotropically. All hydrogen atoms were assigned isotropic displacement coefficients U(H) of 1.2U or 1.5U, and their coordinates were allowed to ride on their respective atoms. The molecule **DCVTT** was found to be a pseudo merohedral twin with a matrix and a BASF parameter of 0.005(2).

$$\begin{pmatrix} 1.934 & 2.508 & -0.402 \\ 1 & -0.5 & 0.5 \\ -0.461 & -0.253 & 0.186 \end{pmatrix}$$

Least-squares refinement of the structural model was performed using restraints (DFIX, RIGU, ISOR, DELU) for the disordered carbon chain and nitrogen atom of nitrile groups.

The molecule crystallizes in the monoclinic space group $P2_1/c$, molecule is shown in SI Fig. 11 (a and b). The ORTEP diagram with 30% ellipsoid is shown in SI Fig. 12. The asymmetric unit contains one molecule of **DCVTT**, and four molecules present in the packing diagram. The intramolecular hydrogen bonding N…S (3.295 Å) as shown in SI Fig. 13 along *b* axis. The molecules have stabilized by packing through the short π…π (3.662 Å) intermolecular interaction between the thiophene ring with each other of head and tail between the molecules. The packing diagram shows the ladder type of network along *c* axis as shown in SI Fig.11 (a and b).

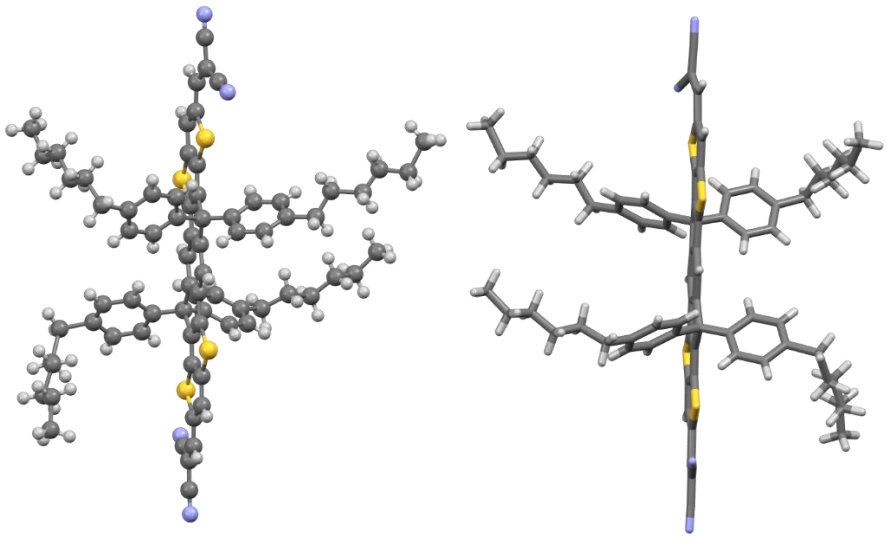

(a) (b)

SI Figure 11: The (a) ball and stick model and (b) capped stick model of the **DCVTT** molecule (C: gray; N: Cyan; S: yellow; H: white)

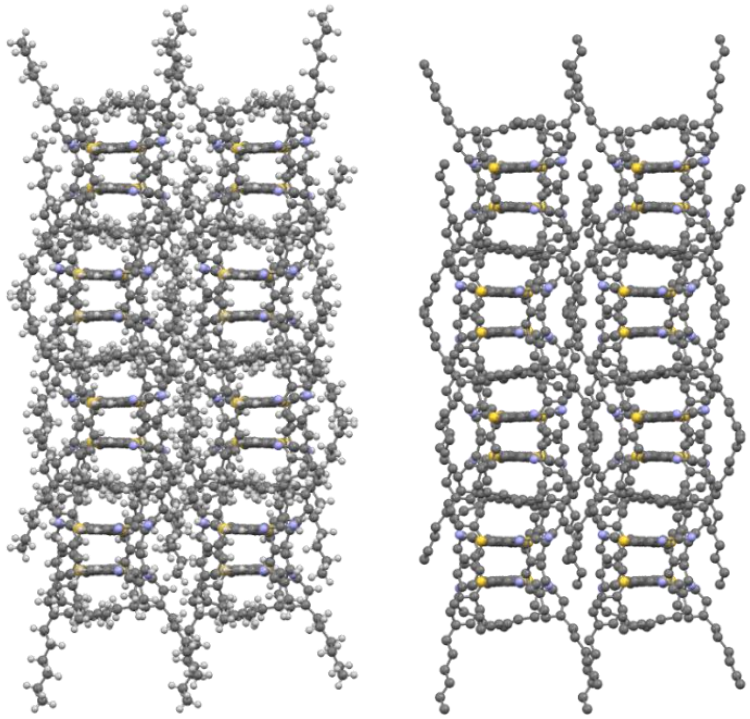

(a) (b)

SI Figure 12: Packing diagram of **DCVTT** molecule along the *c* axis showing (a) extended ladder network (C: gray; N: Cyan; S: yellow; H: white) and (b) without hydrogen atoms showing extended ladder network (C: gray; N: Cyan; S: yellow)

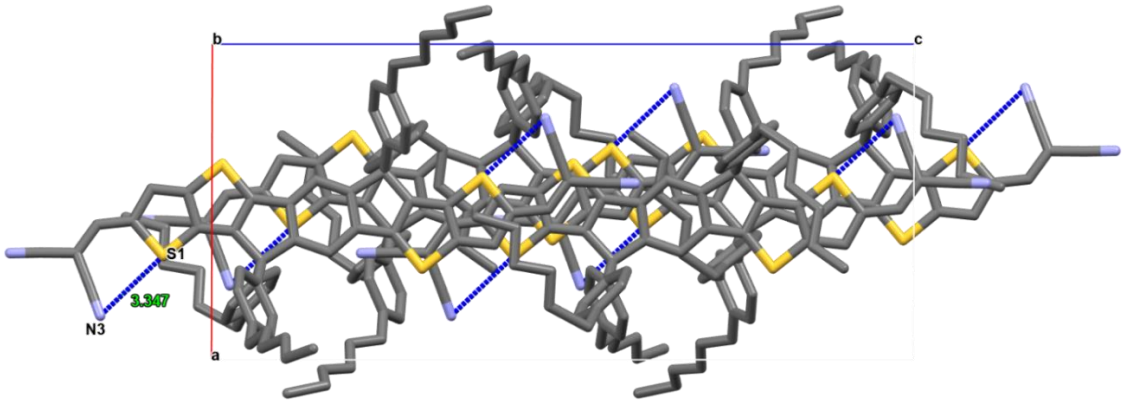

SI Figure 13: Intramolecular hydrogen bonding of **DCVTT** molecule along *b* axis without hydrogen atoms (C: gray; N: Cyan; S: yellow).

SI Table 1. Crystal data and structure refinement for DCVTT.

Crystal data and structure refinement for **DCVTT**	
Identification code	ITDICN
CCDC No.	2344883
Empirical formula	$C_{76}H_{74}N_4S_4$
Formula weight	1171.63
Temperature/K	320.00(10)
Crystal system	monoclinic
Space group	$P2_1/c$
a/Å	12.0240(7)
b/Å	21.0317(15)
c/Å	26.7955(12)
α/°	90
β/°	90.147(5)
γ/°	90
Volume/Å^3	6776.2(7)
Z	4
ρ_{calc}g/cm^3	1.148
μ/mm^{-1}	1.621
F(000)	2488.0
Crystal size/mm^3	0.156 × 0.069 × 0.048
Radiation	Cu Kα (λ = 1.54184)
2Θ range for data collection/°	7.352 to 100.868
Index ranges	-11 ≤ h ≤ 12, 0 ≤ k ≤ 20, 0 ≤ l ≤ 26
Reflections collected	6959
Independent reflections	6959 [R_{int} = ?, R_{sigma} = 0.0931]
Data/restraints/parameters	6959/326/763
Goodness-of-fit on F^2	1.156
Final R indexes [I>=2σ (I)]	R_1 = 0.1185, wR_2 = 0.3109
Final R indexes [all data]	R_1 = 0.1807, wR_2 = 0.3618
Largest diff. peak/hole / e Å^{-3}	0.51/-0.46

ESI Mass spectra of DCVTT in the presence of CN^-

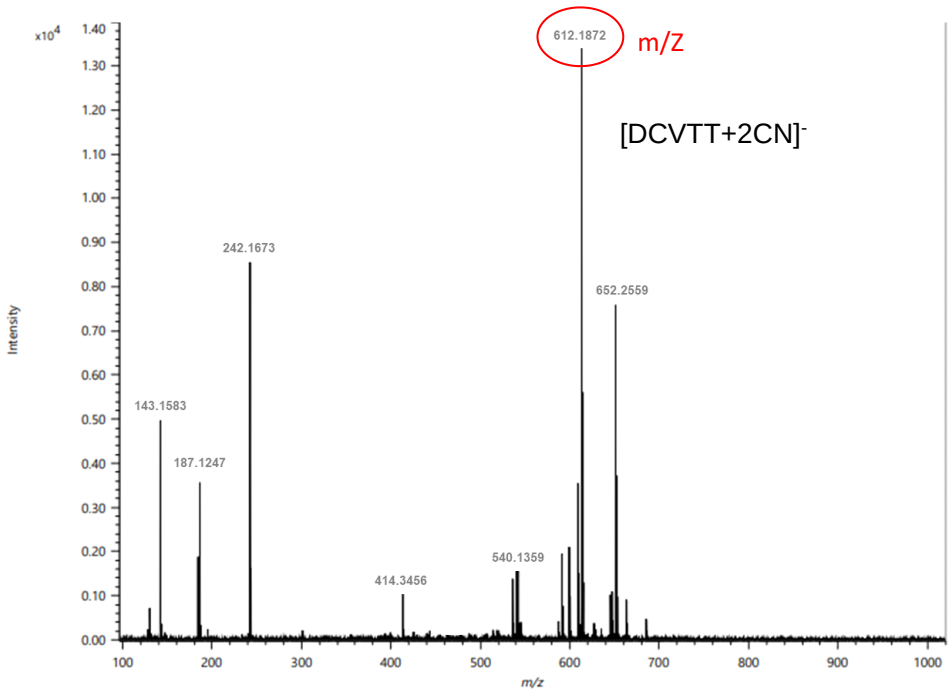

SI Figure 14: ESI Mass spectra of DCVTT in the presence of 10 equivalent of NaCN.

FTIR spectra of DCVTT in the presence and absence of CN^-

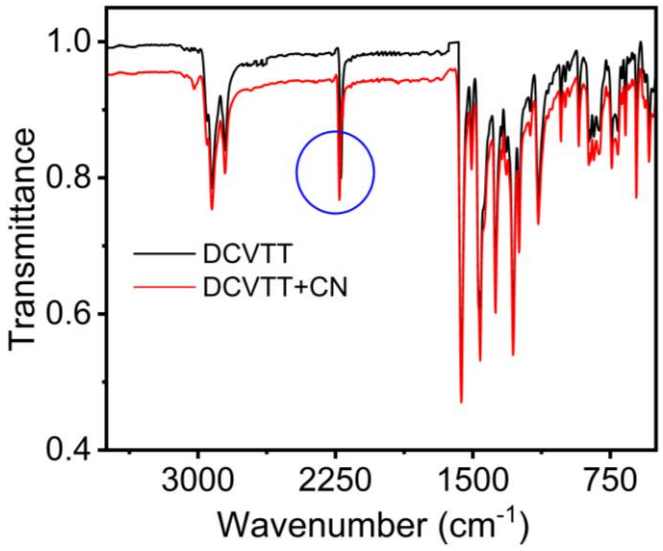

SI Figure 15: FTIR spectra of DCVTT in the presence and absence of 10 equivalent of NaCN in THF/water. Only a very slight shift was observed at CN stretching frequency.

UV-Vis spectral changes of DCVTT in the presence of common metal ions and oxidants

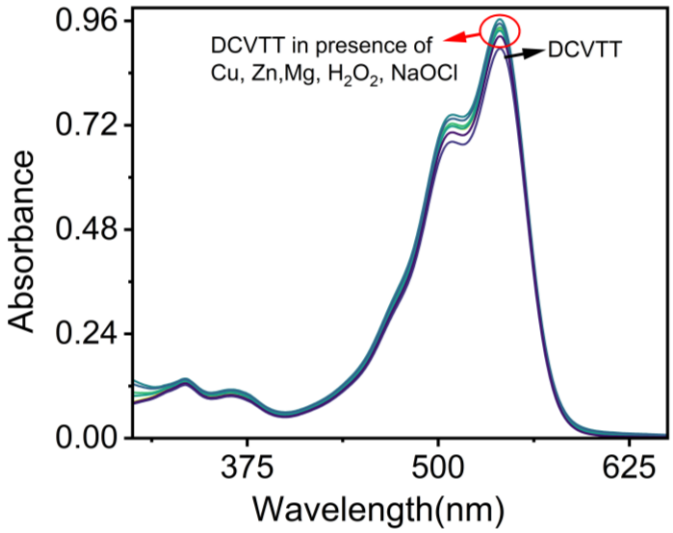

SI Figure 16. Changes in the UV-Vis spectrum of the receptor (**DCVTT**) (20 μM) in the absence and the presence of Cu, Zn, Mg, H_2O_2 and NaOCl (800 μM). All studies were performed in THF: water (1:1).

UV-Vis spectral changes of DCVTT in the presence of Cysteine

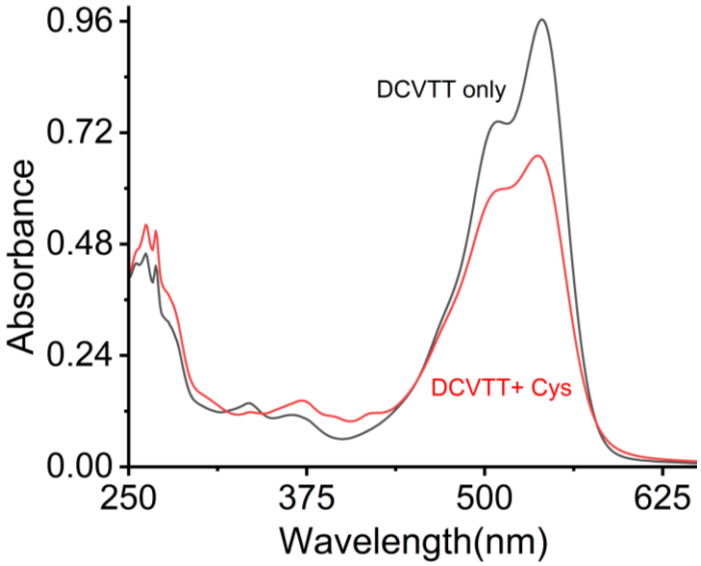

SI Figure 17. Changes in the UV-Vis spectrum of the receptor (**DCVTT**) (20 μM) in the absence and the presence of Cys (50 euiv) was performed in THF: water (1:1).

DFT calculations:

All the geometries were fully optimized using the dispersion-corrected B3LYP-D3[6,7] functional, coupled with the def2-TZVPP[8] basis set. In the solvent, the geometries were optimized with the continuous SMD solvation model.[9] The solvent was modeled of dielectric constants of ε=7.4 (tetrahydrofuran). All calculations were performed using Gaussian 16 program package.[10] The time dependent (TD)-DFT calculations of the complex geometries were performed at the B3LYP-D3/def2-TZVPP level. The lowest 10 vertical excitation energies have been calculated by time-dependent density functional theory (TDDFT) on the optimized geometries.

ICT characteristics of DCVTT were explained by natural transition orbit (NTO) analysis

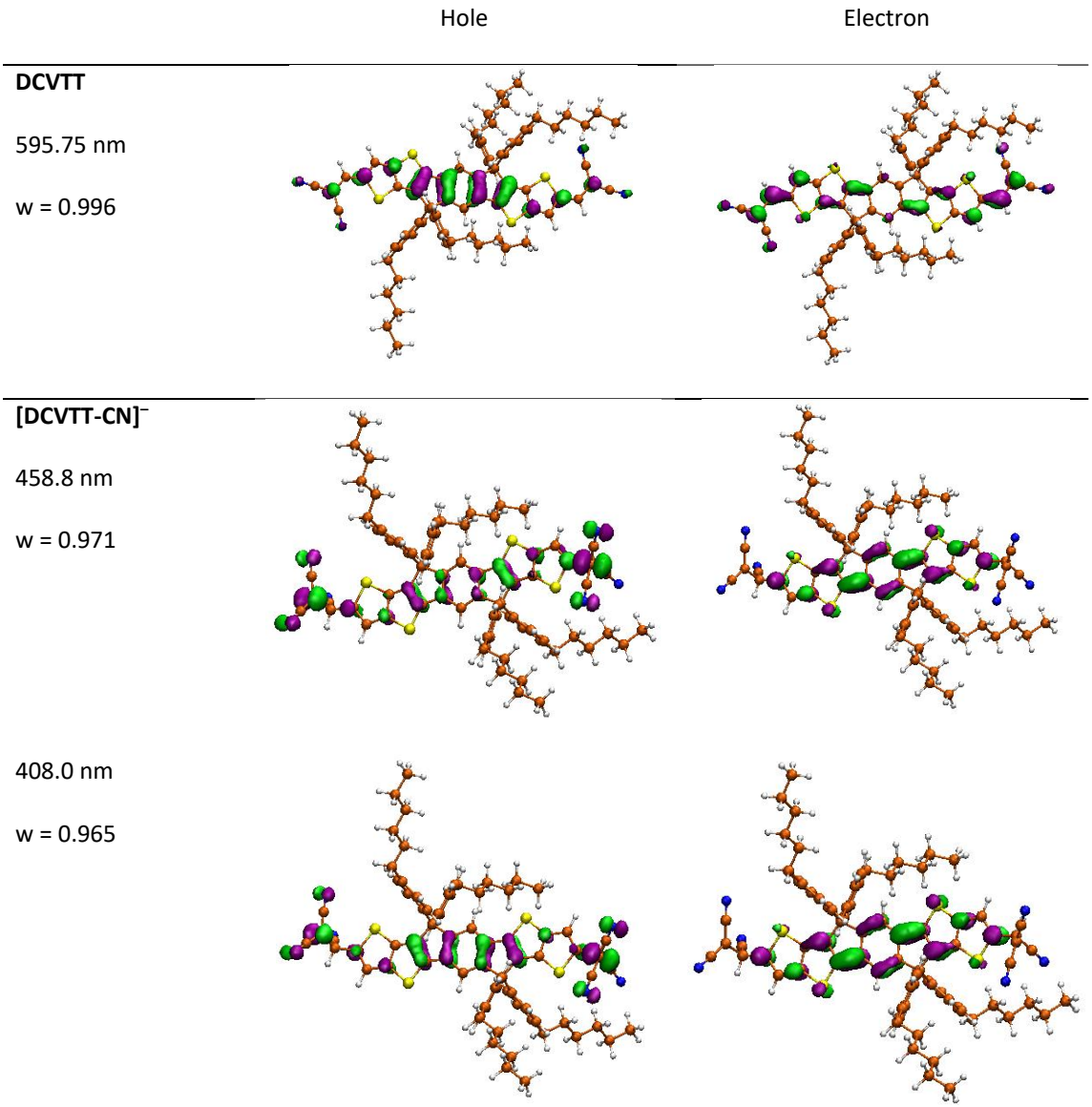

SI Figure 18. Natural transition orbitals (NTOs) for DCVTT and $[DCVTT\text{-}CN]^-$ depict the character of the singlet excited states. For each state, excitation energies (in nm) are provided. Contributions to each excited state are illustrated by NTO pairs for the occupied (hole) and unoccupied (electron) orbitals.[11]

References:

[1] Dolomanov, O.V.; Bourhis, L.J.; Gildea, R.J.;Howard, J.A.K.; & Puschmann, H. J. Appl. Cryst. **2009**, 42, 339-341.

[2] Sheldrick, G.M. Acta Cryst. **2015**, A71, 3-8.

[3] Sheldrick, G.M. Acta Cryst. **2015**, C71, 3-8.

[4] Sheldrick, G. M. Crystal Structure Refinement with SHELXL, *Acta Crystallographica Section C: Structural Chemistry*, **2015**, **71**, 3-8.

[5] Farrugia, L. J. *J. Appl. Crystallogr*. **1997**, 30, 565–565.

[6] (a) Lee, C.; Yang, W.; Parr, R. G., *Phys. Rev. B* **1988**, *37*, 785–789. (b) Becke, A. D *J. Chem. Phys*. **1993**, *98*, 5648–5652.

[7] (a) Grimme, S. *J. Comput. Chem*. **2004**, *25*, 1463-1473. (b) Grimme, S.; Antony, J.; Ehrlich, S.; Krieg, H. H-Pu. *J. Chem. Phys.* **2010**, *132*, 154104. (c) Grimme, S. *WIRES Comput. Mol. Sci.* **2011**, *1*, 211-228. (d) Ehrlich, S.; Moellmann, J.; Grimme, S. *Acc. Chem. Res*. **2012**, *46*, 916-926.

[8] (a) Weigend, F.; Ahlrichs, R. *Phys. Chem. Chem. Phys.* **2005**, *7*, 3297-3305. (b) Weigend, F. *Phys. Chem. Chem. Phys*. **2006**, *8*, 1057-1065.

[9] Marenich, A. V.; Cramer, C. J.; Truhlar, D. G. *J. Phys. Chem. B,* **2009**,*113*, 6378–6396.

[10] Gaussian 16, Revision A.03, Frisch, M. J. et al. Gaussian, Inc., Wallingford CT, **2016**.

[11] Martin, R. L. Natural transition orbitals. J. Chem. Phys. **2003,** 118, 4775–4777.